

## Linear and higher-order power corrections in semileptonic $B$ decays

B. Holdom\* and M. Sutherland†

*Department of Physics, University of Toronto, Toronto, Ontario, Canada M5S 1A7*

(Received 28 April 1993; revised manuscript received 28 July 1993)

In previous work we have developed a relativistic quark model of mesons which is consistent with all QCD constraints at zeroth and first order in the heavy-quark expansion. Here we obtain first-order model predictions for the differential decay spectrum, the forward-backward asymmetry  $A_{FB}$ , and the  $D^*$  polarization parameter  $\alpha$  in the decay  $B \rightarrow D^* \ell \nu$ . We compare these with the predictions of QCD sum rules at first order. The model suggests why the corrections allowed at first order are small, concurrently with substantial corrections at second order.

PACS number(s): 13.20.Jf, 12.40.Aa, 14.40.Jz

### I. INTRODUCTION

We have recently developed a relativistic model for  $B$ -meson semileptonic decays  $B \rightarrow D^{(*)} \ell \nu$ , in which the hadronic matrix elements are represented by quark loop graphs with damping factors at the  $Qq$ -meson vertices [1, 2]. These have the form

$$F_{P,V}(k) = \frac{Z_{P,V}^2}{-k^2 + \Lambda_{P,V}^2}, \quad (1)$$

where  $k$  is the momentum of the light quark and  $P$  and  $V$  denote pseudoscalar and vector mesons. These vertices together with standard quark propagators determine what we will call the “full model,” in which no reference is made to any expansion in inverse powers of heavy-quark masses. The only parameters of the full model are the heavy- and light-quark masses, in terms of which the constants  $\Lambda_{P,V}$  and  $Z_{P,V}$  are fully determined by requiring that the meson self-energy functions vanish and have unit slope at the physically measured meson masses.

We may expand all quantities in the model in inverse powers of heavy-quark masses. Severe constraints on the form of the expansion follow from QCD using the heavy-quark effective theory (HQET) [3]. In the heavy-quark limit, four of the six form factors for  $B \rightarrow D^{(*)} \ell \nu$  become equal to a single universal Isgur-Wise function, while the others vanish [4]. The 12 *a priori* independent  $1/m_c$  and  $1/m_b$  corrections to the form factors are given by specific linear combinations of the Isgur-Wise function and four additional universal functions [5, 6]. The actual shapes of these universal functions are model dependent, but some have model-independent values at zero recoil. We have shown in [1] that all such constraints are satisfied by our model at first order.

The HQET restrictions arising at second order ( $1/m_Q^2$ ) are available in [7]. We have not yet demonstrated consistency with these results, as our model for mesons is

rather unwieldy at this order. On the other hand we have developed a similar model for  $\Lambda_Q$  baryons [8]. It is more tractable than the meson case and is fully consistent with the HQET constraints presented in [9] up to and including second order. Our approach for mesons follows the same principles and we thus conjecture that it is also consistent at second order.

As was shown in [2], the main feature of the full model before expansion is the presence of rather large deviations from the heavy-quark limit predictions for the zero-recoil values of the form factors  $h_+$  and  $h_{A_1}$ , defined in Eqs. (A5) and (A9) below. These quantities play a crucial role in the determination of the Kobayashi-Maskawa element  $V_{cb}$ , as discussed in [10]. Both are equal to 1 in the heavy-quark limit and neither receives corrections at order  $1/m_Q$  (Luke’s theorem [5]). The corrections we found were traced to the effects of hyperfine mass splitting. For the choice of quark masses in [2] we found values of 10–15% for the corrections at all orders, with the corrections occurring purely at second order making up about 2/3 of these full corrections. This translates almost directly into a 10–15% model dependence in  $V_{cb}$ .

We believe that it is currently of interest to obtain estimates of the corrections beyond first order in  $1/m_Q$  in any model, such as ours, which is consistent with the heavy-quark symmetries. Many of the previously popular models [11–13] cannot be used since they do not obey the symmetry constraints, as described in [14]. Of course the question remains as to how well our model resembles QCD. Perhaps the main question has to do with confinement; our representation of the effects of confinement is to simply ignore the imaginary parts arising from our free quark loop calculations. We emphasize again, though, that this procedure is consistent with Ward identities and heavy-quark symmetries [1].

Another approach [7] has been to carefully study the structure of the second-order corrections in the HQET. Here the question boils down to the estimation of matrix elements of various operators. Sum rules have been applied to the first-order corrections, but the estimates of the second-order corrections are much less sophisticated. In [7] some matrix elements are estimated using the Isgur-Scora-Grinstein-Wise (ISGW) nonrelativistic quark model [11], but this model does not include hy-

\*Electronic address: holdom@utcc.utoronto.ca

†Electronic address: marks@medb.physics.utoronto.ca

perfine splitting effects. In fact when hyperfine splitting effects are turned off in our model [i.e., when  $g = h = 0$  in (2) below] we find order  $1/m_Q^2$  contributions to  $h_+$  and  $h_{A_1}$  at zero recoil which are very similar to those of the ISGW model.

Other matrix elements involve double insertions of the chromomagnetic moment operator, and these are neglected in [7] since the single insertions appearing at first order are observed to be small. But these double insertion matrix elements are precisely the ones which are large in our model [2], and they are large concurrently with small values for the single insertion matrix elements. We will argue below that the small size of the first-order corrections to semileptonic decay amplitudes is the exception rather than the rule. The suggested mechanism that suppresses the first-order corrections does not apply to higher-order corrections. Even at first order large corrections are possible; for example our model and sum rules agree that the heavy meson decay constants receive much larger first-order corrections than the semileptonic decay amplitudes [1].

Until more reliable estimates of the second-order corrections appear, our model gives some indication of the possible theoretical uncertainty in the extraction of  $V_{cb}$ . One of the objects of this paper is to provide a set of model predictions to be compared to future data. In particular we will define a “first-order model” in which only the first-order corrections are kept, and we consider quantities which are fairly insensitive to the higher-order corrections. We compare these results with QCD sum rules [15] and find that the differences may be large enough to make the two first-order models experimentally distinguishable. We will also see from the present data that drastic modifications to the model cannot be tolerated.

In the last part of the paper we shall develop more understanding of the higher-order corrections found in the full model. We will stress the consequences of holding the physical meson masses fixed in the full model, in particular constraints on  $m_c$  and  $m_b$ .

## II. THE FIRST-ORDER MODEL

The first-order model has three parameters, in addition to the quark masses. The heavy-quark limit  $m_Q \rightarrow \infty$  is characterized uniquely by the ratio  $\Lambda/m_q$ , where  $m_q$  is the light-quark mass and  $\Lambda$  is the common value of  $\Lambda_{P,V}$  in the heavy-quark limit. The other two parameters  $g$  and  $h$  characterize the approach to the heavy-quark limit via

$$\Lambda_{P,V} = \Lambda \left( 1 - (\delta_{P,V} h + g) \frac{\Lambda}{m_Q} \right), \quad (2)$$

where  $\delta_P = 3$  and  $\delta_V = -1$ .<sup>1</sup> The bulk of hyperfine mass splitting is contained in  $h$ , a positive value of which drives the pseudoscalar mass down and the vector mass up by amounts in the ratio of 3 to 1. But not all effects of the heavy-quark spin-symmetry breaking are described by  $h$ ;

some breaking is intrinsic to the relativistic quark loop and it is present when  $h = 0$ . The three parameters of the first-order model are free parameters, and the consistency with heavy-quark symmetry is valid for any values of these parameters.

For the purpose of computing physical predictions with the first-order model, numerical values of its parameters may be estimated as follows. As in [1, 2], we choose  $m_b = 4.8$  GeV,  $m_c = 1.44$  GeV, and  $m_q = 250$  MeV. The first-order model then yields expressions for the  $B$ ,  $B^*$ ,  $D$ , and  $D^*$  masses in terms of  $\Lambda$ ,  $g$ , and  $h$ . These we adjust to fit the four masses, yielding an optimal mass spectrum when  $\Lambda = 667$  MeV,  $g = -0.13$ , and  $h = 0.19$ . In this way the model is fixed once the quark masses are given, and we find that changes in the first-order results are minor for any reasonable choice of quark masses.

The mass difference between the meson and the heavy quark in the heavy-quark limit is denoted by  $\bar{\Lambda}$  [16]; it is directly related to  $\Lambda$  [1]. With the above values of  $\Lambda$  and  $m_q$ , we have  $\bar{\Lambda} = 504$  MeV, which coincides with the QCD sum rule estimate in [15]. In addition, the Isgur-Wise function from this model is numerically very similar to one given in a sum rule analysis [17]:

$$\xi(\omega)^{\text{s.r.}} = \left( \frac{2}{\omega + 1} \right)^{1.88 + \frac{0.69}{\omega}}. \quad (3)$$

The slope at  $\omega = 1$  is  $-1.28$ .<sup>2</sup>

As mentioned above, four additional universal functions  $\chi_1$ ,  $\chi_2$ ,  $\chi_3$ , and  $\xi_3$  appear at first order [5, 16]. Their values are plotted for the above parameter values in Fig. 1. All are relatively small compared with the Isgur-Wise function, which is 1 at zero recoil and approximately 0.6 at  $\omega = 1.5$ . In fact we can begin to see how it is that dimensionless quantities appearing at first order are small compared to unity.  $\chi_2$  and  $\xi_3$  are spin-symmetry violating and conserving, respectively, but they are both independent of the parameters  $g$  and  $h$  for any  $\omega$  [1]. They are therefore independent of the “wave function” distortions described by  $g$  and  $h$  which are required to fit the physical meson masses.  $\chi_1$  is spin-symmetry conserving and therefore depends only on  $g$  while  $\chi_3$  is spin-symmetry violating and depends only on  $h$ . But both  $\chi_1$  and  $\chi_3$  are constrained to be zero at zero recoil by Luke’s theorem, and thus for the physical range of  $\omega$  they remain small. There is thus no quantity at first order which is both sensitive to “wave function” distortions and nonvanishing at zero recoil. In contrast, there are such dimensionless quantities appearing at second order in the heavy-quark expansion [2]. Such quantities can be expected to be of order unity, and they thereby give corrections which appear to be large when compared to the first-order corrections.

Since  $\chi_2$  and  $\xi_3$  are independent of the parameters  $g$  and  $h$  the following combinations of  $B \rightarrow D^*$  form factors are especially interesting:

<sup>1</sup>The definition of  $g$  and  $h$  here differs from that in [1].

<sup>2</sup>More recent sum rule analyses favor a less negative slope [14].

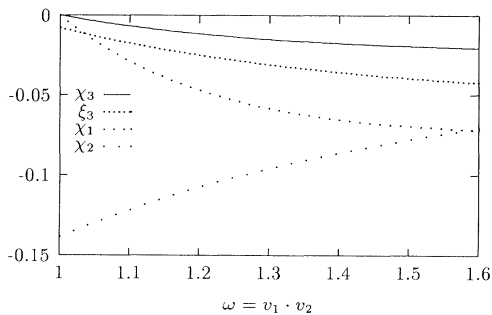


FIG. 1. First-order model predictions for universal functions  $\xi_3$  and  $\chi_{1,2,3}$  for  $\Lambda = 667$  MeV,  $m_q = 250$  MeV,  $g = -0.13$ , and  $h = 0.19$ .

$$R_1 = \frac{h_V}{h_{A_1}} \approx 1 + \frac{1}{\omega + 1} \left[ \frac{\bar{\Lambda}}{m_c} + \frac{\bar{\Lambda}}{m_b} \left( 1 - 2 \frac{\xi_3}{\xi} \right) \right], \quad (4)$$

$$R_2 = \frac{h_{A_3} + (m_{D^*}/m_B)h_{A_2}}{h_{A_1}} \approx 1 + \frac{1}{\xi} \left\{ \frac{\bar{\Lambda}}{m_c} \left( \frac{-\xi_3}{1+\omega} - 2\chi_2 \right) + \frac{\bar{\Lambda}}{m_b} \left( \frac{-3\xi_3}{1+\omega} + 2\chi_2 \right) \right\}. \quad (5)$$

These quantities have also been stressed elsewhere [15]. Both  $R_1$  and  $R_2$  are nearly constant across the spectrum. The main difference with QCD sum rules is that our  $\xi_3$  is much smaller. Our result  $R_1 \approx 1.3$  is still in agreement with QCD sum rules due to the  $1/m_b$  suppression of the second term. But  $R_2 \approx 1.0$  differs somewhat from the value of 0.8 found in QCD sum rules [14].

Indeed we find, in contrast to the Isgur-Wise function, that all four universal functions arising at first order in our model are rather different from those in QCD sum rules, and that they lead to different physical predictions. For example, we may consider the differential  $B \rightarrow D^*$  spectrum in  $\omega$ . In the heavy-quark limit this goes over to  $|V_{cb}|^2 g(\omega) \xi(\omega)^2$  where  $g(\omega)$  is a known function of the

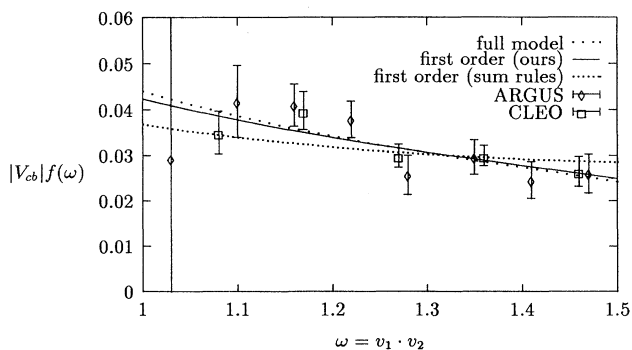


FIG. 2. Predictions for the  $B \rightarrow D^*$  spectrum  $|V_{cb}|f(\omega)$  [equal to  $|V_{cb}|\xi(\omega)$  in the heavy-quark limit]. The respective values of  $|V_{cb}|$  are 0.042 in our first order model, 0.037 in first-order QCD sum rules, and 0.038 in our full model.

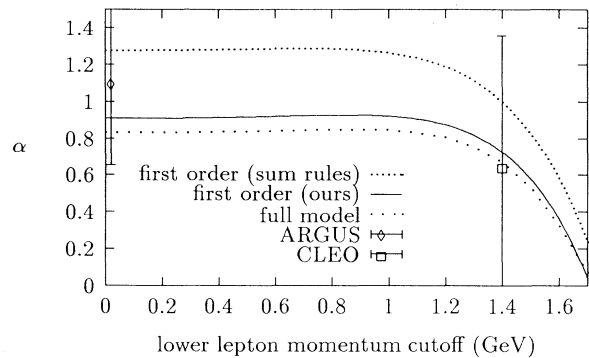


FIG. 3.  $D^*$  polarization parameter  $\alpha$  as a function of the experimental lower lepton momentum cut  $p_{\text{cut}}$ .

meson masses and includes short distance QCD corrections. (We include short-distance QCD corrections [15] in all subsequent computations.) Dividing the spectrum by  $g(\omega)$  and taking the square root then yields  $|V_{cb}|f(\omega)$  where  $f(\omega)$  goes over to  $\xi(\omega)$  in the heavy-quark limit. The first-order model predicts  $f(\omega)$ , and we obtain  $|V_{cb}|$  by fitting to the data.

This raises an important point. The normalization  $f(1) = 1$  at first order is model independent, so it would be possible to obtain  $|V_{cb}|$  in a model-independent way if there were data at zero recoil. But the differential spectrum vanishes at zero recoil, so we require an extrapolation. This extrapolation can only be accomplished by fitting some functional form to the data; this functional form is model dependent and hence so is  $|V_{cb}|$ . This model dependence will diminish only as the data improves.

We plot in Fig. 2 the first-order model results together with ARGUS [18] and CLEO [19] data for  $|V_{cb}|f(\omega)$ . We see that the shape of our curve is steeper than that predicted by QCD sum rules, and that the present data favor the steeper curve. At first order  $f(1) = 1$ , so  $|V_{cb}|$  may simply be read off as the intercept of the curve. We find  $|V_{cb}| = 0.042$  in our model and  $|V_{cb}| = 0.037$  in QCD sum

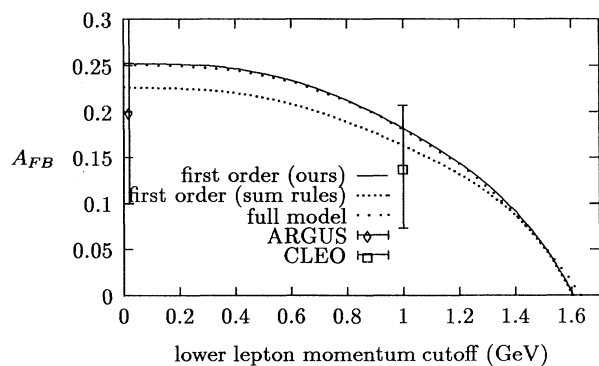


FIG. 4. Forward-backward asymmetry  $A_{FB}$  in the angle  $\theta$ , as a function of the lepton momentum cut. The cut is performed symmetrically as explained in the text.

rules, a difference of 13%. This large discrepancy is due entirely to the first-order corrections, since we have used the same Isgur-Wise function for both cases.

We next present results for two integrated quantities which directly sample the data away from zero recoil: the  $D^*$  polarization parameter  $\alpha$  and the forward-backward asymmetry  $A_{FB}$ . These are plotted versus the experimental lepton momentum cut in Figs. 3 and 4. The present experimental values [18, 20, 21] of  $A_{FB}$  and  $\alpha$  are also displayed. In both cases, the predictions of our first-order model differ from those of QCD sum rules; better data would make it possible to distinguish between them.

### III. THE FULL MODEL

If we consider the same quark masses as above then the full model yields [2]  $h_+(1) = 1.107$  and  $h_{A_1}(1) = 1.155$ , in contrast with their model-independent values of 1 at first order. The value of  $|V_{cb}|$  is then no longer given by the intercept of the full model curve shown in Fig. 2, and  $|V_{cb}|$  in this case is 0.38. In contrast, the effects of these higher-order corrections manifest themselves only slightly in  $\alpha$ , as shown in Fig. 3. And as seen in Fig. 4 they cancel out almost completely in  $A_{FB}$ .

We now turn to a discussion of the sensitivity of the full model results to the heavy-quark masses. By fixing the physical values of the meson masses, the quantities  $Z_{P,V}$  and  $\Lambda_{P,V}$  of Eq. (1) are fully determined for each meson, as mentioned at the outset. This points to a fundamental difference in the interpretation of the full model versus the heavy-quark expansion. In the latter, the meson masses vary as the heavy-quark mass varies. But in the full model the physical meson masses are held fixed. Then the dependence of various quantities on the heavy-quark mass has no connection with the standard dependence in the heavy-quark expansion. In fact in the full model it will only be possible to produce physical meson masses when the quark masses are within some range. This is a feature of any realistic model of QCD for fixed hadron masses. In fact, the better the model, the more the quark masses should be constrained to their true values.

We can capitalize on this fact and use the full model to constrain  $m_c$  and  $m_b$ . An easily measurable quantity which has strong dependence on these masses is the ratio of branching ratios  $B(B \rightarrow D)/B(B \rightarrow D^*)$ . We illustrate this by plotting this ratio in Fig. 5 as a function of  $m_c$  at fixed  $m_b = 4.8$  GeV (with no lepton momentum cut). As the data improve this mass dependence will translate into a constraint on  $m_c$  as a function of  $m_b$ .

In fact, constraints on the heavy-quark masses already arise. We consider both  $B \rightarrow D^*$  and  $B \rightarrow D$  processes and we find that the allowed region in the  $m_c$ - $m_b$  plane is defined by

$$m_c + \Lambda_B(m_b; m_q) > M_{D^*}, \quad (6)$$

$$m_b + \Lambda_D(m_c; m_q) > M_B. \quad (7)$$

This allowed region is displayed in Fig. 6 for a light-quark mass  $m_q = 250$  MeV. These conditions may be understood by considering the form of the damping fac-

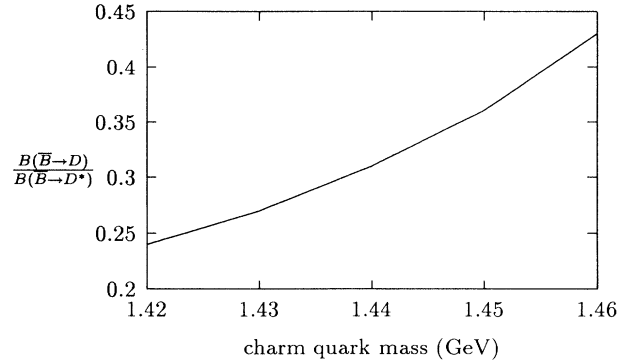


FIG. 5. Full model prediction for  $B(B \rightarrow D)/B(B \rightarrow D^*)$  as a function of the charm quark mass with bottom quark mass fixed at 4.8 GeV.

tor in (1). They ensure that the  $D^*$  is below threshold to produce a free charm quark and an unphysical particle with mass  $\Lambda_B$ , and that the  $B$  is below threshold to produce a free bottom quark and an unphysical particle with mass  $\Lambda_D$ . (Other conditions such as  $m_c + \Lambda_B > M_D$  and  $m_b + \Lambda_{D^*} > M_B$  are less restrictive.) As we have said, the existence of an allowed region is expected due to the fact that the meson masses are fixed.

Our canonical choice  $m_c = 1.44$  GeV and  $m_b = 4.80$  GeV lies close to a line running down the middle of the allowed region. The corrections to the  $B \rightarrow D^*$  form factors increase as the point  $(m_c, m_b)$  gets closer to the constraint (6) involving  $M_{D^*}$ , and the corrections to the  $B \rightarrow D$  form factors increase as the point gets closer to the constraint (7) involving  $\Lambda_D$ . This effect manifests itself as the anticorrelation in the full model predictions for the branching ratios, as seen in Fig. 5. As another illustration we show in Fig. 7 the corrections to  $h_{A_1}(1)$  and  $h_+(1)$  as functions of  $m_c$  with  $m_b = 4.8$  GeV held fixed. We again see the anticorrelation in the corrections.

It is of interest that for no reasonable choices of quark masses are the corrections to  $h_{A_1}(1)$  and  $h_+(1)$  small simultaneously. In [2] we associated these corrections with hyperfine splitting effects. This may be rephrased in the language of Fig. 6 with the aid of Table 1 in [2]. There

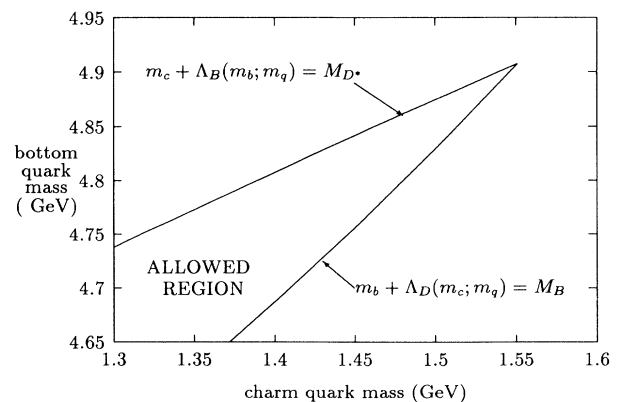


FIG. 6. Allowed region in the  $m_c$ - $m_b$  plane, for light-quark mass  $m_q = 250$  MeV.

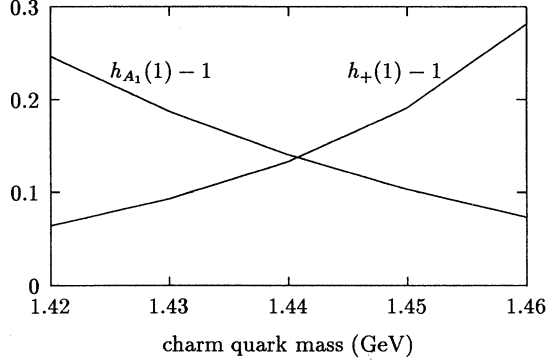


FIG. 7. Full model results for  $h_{A_1}(1)$  and  $h_+(1)$  as functions of the charm quark mass with bottom quark mass fixed at 4.8 GeV.

it is seen that both  $M_{D^*} - \Lambda_B$  and  $M_B - \Lambda_D$  decrease when hyperfine mass splitting is turned off. From (6) and (7) this has the effect of enlarging the allowed region in the  $m_c$ - $m_b$  plane, and the corrections are correspondingly reduced.

It may seem most reasonable for the corrections to  $h_{A_1}(1)$  and  $h_+(1)$  to be of the same order of magnitude, and thus both in the 10–15% range. A more precise statement awaits more experimental input, as we have described. The main point of this paper has been to obtain definite predictions for other quantities, and how these predictions fare will determine how seriously this model should be taken.

#### ACKNOWLEDGMENTS

This research was supported in part by the Natural Sciences and Engineering Research Council of Canada. B.H. thanks A. Falk and M. Luke for useful discussions; he also thanks the Aspen Center for Physics where this work was completed.

#### APPENDIX

We summarize in this appendix the definitions of all relevant quantities. The full fourfold decay distribution in the cascade decay  $\bar{B}^0 \rightarrow D^{*+}(\rightarrow D\pi) + \ell^- + \bar{\nu}_\ell$  may be written as [22]

$$\frac{d\Gamma[\bar{B}^0 \rightarrow D^{*+}(\rightarrow D\pi)\ell^-\bar{\nu}_\ell]}{d\omega d\cos\theta d\cos\theta^* d\chi} = B(D^{*+} \rightarrow D\pi) \sum_i \frac{f_i(\theta, \theta^*, \chi)}{2\pi} \frac{d\Gamma_i(\omega)}{d\omega}. \quad (\text{A1})$$

$$\langle D^* | \bar{c}\gamma_\mu b | \bar{B}^0 \rangle = \sqrt{M_1 M_2} h_V(\omega) \varepsilon_{\mu\nu\rho\sigma} \varepsilon_2^{*\nu} v_2^\rho v_1^\sigma, \quad (\text{A4})$$

$$\langle D^* | \bar{c}\gamma_\mu \gamma_5 b | \bar{B}^0 \rangle = -i\sqrt{M_1 M_2} [(\omega + 1)h_{A_1}(\omega)\varepsilon_{2\mu}^* - (h_{A_2}(\omega)v_{1\mu} + h_{A_3}(\omega)v_{2\mu})\varepsilon_2^* \cdot v_1], \quad (\text{A5})$$

where  $\varepsilon_2$  is the  $D^*$  polarization vector. The three helicity amplitudes are given in terms of the four form factors by

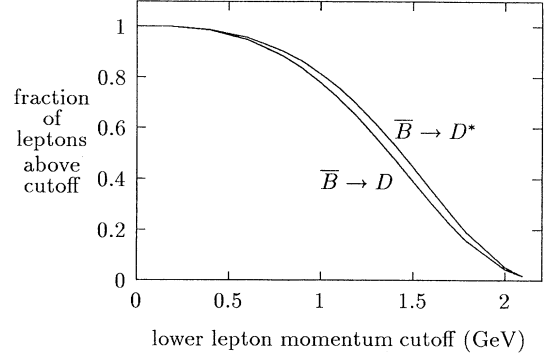


FIG. 8. Full model prediction for fraction of leptons having momentum greater than a given minimum value.

$\theta$  is the polar angle of the lepton measured with respect to the  $D^*$  direction in the  $(\ell\bar{\nu}_\ell)$  c.m. system,  $\theta^*$  is the polar angle of the  $D$  relative to the  $D^*$  in the  $D^*$  rest frame, and  $\chi$  is the azimuthal angle between the two decay planes spanned by  $(D\pi)$  and  $(\ell\bar{\nu}_\ell)$ . See [22, 18] for diagrams.  $B(D^{*+} \rightarrow D\pi)$  is the branching ratio  $\Gamma_{D^{*+} \rightarrow D\pi} / \Gamma_{D^{*+} \rightarrow \text{all}}$ . The zero lepton mass approximation has been used. The angular functions  $f_i$  are listed in (A2):

$i$	$f_i$	$\hat{H}_i$
$U$	$\frac{9}{32}(1 + \cos^2\theta)\sin^2\theta^*$	$\frac{ H_+ ^2 +  H_- ^2}{ H_0 ^2}$
$L$	$\frac{9}{8}\sin^2\theta\cos^2\theta^*$	$ H_0 ^2$
$T$	$-\frac{9}{16}\sin^2\theta\sin^2\theta^*\cos 2\chi$	$\text{Re}(H_+H_-^*)$
$I$	$-\frac{9}{16}\sin 2\theta\sin 2\theta^*\cos \chi$	$\frac{1}{2}\text{Re}(H_+H_0^* + H_-H_0^*)$
$P$	$\frac{9}{16}\cos\theta\sin^2\theta^*$	$ H_+ ^2 -  H_- ^2$
$A$	$-\frac{9}{8}\sin\theta\sin 2\theta^*\cos \chi$	$\frac{1}{2}\text{Re}(H_+H_0^* - H_-H_0^*)$

(A2)

The partial helicity rates  $d\Gamma_i/d\omega$  are given by

$$\frac{d\Gamma_i}{d\omega} = \frac{G_F^2 |V_{cb}|^2}{48\pi^3} M_1 M_2^2 \sqrt{\omega^2 - 1} (1 + r^2 - 2r\omega) \hat{H}_i(\omega), \quad (\text{A3})$$

where  $M_{1,2}$  are the  $\bar{B}^0$  and  $D^*$  masses and  $r = M_2/M_1$ .  $\hat{H}_i$  are bilinear expressions of the three helicity amplitudes  $H_+$ ,  $H_-$ , and  $H_0$  describing the current-induced transitions  $B \rightarrow D^*$ , and are listed in (A2). A set of four form factors may be defined by

$$\begin{aligned}
H_{\pm} &= \sqrt{M_1 M_2} (\omega + 1) \{h_{A_1} \mp [(\omega - 1)/(\omega + 1)]^{1/2} h_V\}, \\
H_0 &= \frac{\sqrt{M_1 M_2} (\omega + 1)}{\sqrt{1 + r^2 - 2r\omega}} \{(\omega - r)h_{A_1} - (\omega - 1)(h_{A_3} + r h_{A_2})\}.
\end{aligned} \tag{A6}$$

The differential decay rate for  $\overline{B^0} \rightarrow D^+ + \ell + \bar{\nu}_\ell$  is given by [13]

$$\frac{d\Gamma(\overline{B^0} \rightarrow D^+ \ell \bar{\nu}_\ell)}{d\omega d\cos\theta} = \frac{3}{4} (1 - \cos^2\theta) \frac{d\Gamma}{d\omega}, \tag{A7}$$

where

$$\frac{d\Gamma}{d\omega} = \frac{G_F^2 |V_{cb}|^2}{48\pi^3} M_1 M_2^2 \sqrt{\omega^2 - 1} (1 + r^2 - 2r\omega) |H_0^D(\omega)|^2. \tag{A8}$$

$M_2$  is now the  $D$  mass. The standard pair of form factors are defined by

$$\langle D | \bar{c} \gamma_\mu b | \overline{B^0} \rangle = \sqrt{M_1 M_2} [h_+(\omega)(v_1 + v_2)_\mu + h_-(\omega)(v_1 - v_2)_\mu]. \tag{A9}$$

The amplitude  $H_0^D$  is given in terms of  $h_{\pm}$  by

$$H_0^D = \frac{\sqrt{M_1 M_2} \sqrt{\omega^2 - 1}}{\sqrt{1 + r^2 - 2r\omega}} \{(1 + r)h_+ - (1 - r)h_-\}. \tag{A10}$$

The total of six form factors have the following values in the heavy-quark limit:

$$h_{V, A_1, A_3, +} = \xi, \quad h_{A_2, -} = 0. \tag{A11}$$

In all of the model results quoted we include short distance QCD corrections  $\beta_i(\omega)$  [15] according to

$$h_i(\omega)^{\text{QCD}} = h_i(\omega)^{\text{no QCD}} + \beta_i(\omega)\xi(\omega). \tag{A12}$$

We implement the momentum cut according to the prescription set out in [22]; in our notation, this reads

$$-1 \leq \cos\theta \leq \min(\cos\theta(\omega; p_{\text{cut}}), 1) \tag{A13}$$

where

$$\cos\theta(\omega; p_{\text{cut}}) = \frac{1 - r\omega - 2p_{\text{cut}}/M_1}{r\sqrt{\omega^2 - 1}}. \tag{A14}$$

When converting data into values for branching ratios,

the events lost due to the cut must be restored. In order to facilitate this we plot in Fig. 8 the full model prediction for the fraction of leptons having momentum greater than the cut, for  $B \rightarrow D$  and  $B \rightarrow D^*$ . This fraction is quite insensitive to  $m_c$ .

In uncut form, the forward-backward asymmetry in the angle  $\theta$  is given by

$$A_{\text{FB}} = -\frac{3}{4} \frac{\Gamma_P}{\Gamma_U + \Gamma_L}, \tag{A15}$$

where

$$\Gamma_i = \int_1^{\omega_{\text{max}}} d\omega \frac{d\Gamma_i}{d\omega}, \quad \omega_{\text{max}} = \frac{1 + r^2}{2r}. \tag{A16}$$

The lepton momentum cut excludes events in the extreme backward direction  $\cos\theta \rightarrow 1$ ; following [22] we remove this bias by symmetrizing the definition of  $A_{\text{FB}}$  with the forward hemisphere restricted by

$$-\min(\cos\theta(\omega; p_{\text{cut}}), 1) \leq \cos\theta \leq 0. \tag{A17}$$

In uncut form, the  $D^*$  polarization parameter is given by

$$\alpha = 2 \frac{\Gamma_L}{\Gamma_U} - 1. \tag{A18}$$

- 
- |   |   |
|---|---|
| <p>[1] B. Holdom and M. Sutherland, Phys. Rev. D <b>47</b>, 5067 (1993).</p> <p>[2] B. Holdom and M. Sutherland, Phys. Lett. B <b>313</b>, 447 (1993).</p> <p>[3] H. Georgi, Phys. Lett. B <b>240</b>, 447 (1990).</p> <p>[4] N. Isgur and M.B. Wise, Phys. Lett. B <b>232</b>, 113 (1989); <b>237</b>, 527 (1990).</p> <p>[5] M.E. Luke, Phys. Lett. B <b>252</b>, 447 (1990).</p> <p>[6] M. Neubert and V. Rieckert, Nucl. Phys. <b>B382</b>, 97 (1992).</p> <p>[7] A.F. Falk and M. Neubert, Phys. Rev. D <b>47</b>, 2965 (1993).</p> <p>[8] B. Holdom and M. Sutherland, University of Toronto Report No. UTPT-93-26, 1992 (unpublished).</p> <p>[9] A.F. Falk and M. Neubert, Phys. Rev. D <b>47</b>, 2982 (1993).</p> <p>[10] M. Neubert, Phys. Lett. B <b>264</b>, 455 (1991).</p> <p>[11] N. Isgur, D. Scora, B. Grinstein, and M. Wise, Phys. Rev. D <b>39</b>, 799 (1989).</p> <p>[12] M. Wirbel, B. Stech, and M. Bauer, Z. Phys. C <b>29</b>, 637 (1985).</p> | <p>[13] J.G. Körner and G.A. Schuler, Z. Phys. C <b>38</b>, 511 (1988); <b>41</b>, 690(E) (1989); <b>46</b>, 93 (1990).</p> <p>[14] M. Neubert, Phys. Rep. (to be published).</p> <p>[15] M. Neubert, Phys. Rev. D <b>46</b>, 3914 (1992).</p> <p>[16] A. Falk, M. Neubert, and M. Luke, Nucl. Phys. <b>B388</b>, 363 (1992).</p> <p>[17] M. Neubert, Phys. Rev. D <b>45</b>, 2451 (1992).</p> <p>[18] ARGUS Collaboration, H. Albrecht, in <i>Proceedings of the 26th International Conference on High Energy Physics</i>, Dallas, Texas, 1992, edited by J. Sanford, AIP Conf. Proc. No. 272 (AIP, New York, 1993).</p> <p>[19] D. Bortoletto and S. Stone, Phys. Rev. Lett. <b>65</b>, 2951 (1990).</p> <p>[20] CLEO Collaboration, D. Bortoletto <i>et al.</i>, Phys. Rev. Lett. <b>63</b>, 1667 (1989).</p> <p>[21] CLEO Collaboration, S. Sanghera <i>et al.</i>, Phys. Rev. D <b>47</b>, 791 (1993).</p> <p>[22] J.G. Körner and G.A. Schuler, Phys. Lett. B <b>226</b>, 185 (1989).</p> |
|---|---|